

“MONITORING THE LARGEST NORTH KOREAN NUCLEAR EXPLOSION 2017, THROUGH INDIAN SEISMOLOGICAL NETWORK”

Sanjay Kumar Prajapati^{1,*}, Rajesh Prakash¹, and Hari Narain Srivastava²

⁽¹⁾ National Centre for Seismology, New Delhi, India

⁽²⁾ Ex-Additional Director General, India Meteorological Department, New Delhi, India

Article history

Received November 19, 2018; accepted March 15, 2019.

Subject classification:

North Korea nuclear test 2017; Seismic network; mb versus Ms; Source mechanism; Waveform modelling.

ABSTRACT

Seismological characteristics of the North Korean largest nuclear test of September 2017 have been examined using the data of the Indian Seismological Network. Full waveform modelling of the ground motion data of Indian stations for this nuclear test shows 16% isotropic component, 47.5% DC and 35.8% CLVD components. The Indian stations being located about 3500 to 5000 km away from the source, gave lesser isotropic component as compared to that from the nearby stations around the North Korean test site. This is attributed to the rapid attenuation of the high frequencies emitted from the source. Its average body wave magnitude, mb from the Indian stations broadly agrees with that reported by worldwide data. It was found that the surface wave magnitude of this test in North Korea was large as compared to those from the Kazakhstan and Nevada nuclear tests for almost similar mb. It is hypothesized that more powerful fusion process in the nuclear test could result in larger tectonic slip.

1. INTRODUCTION

North Korea nuclear test of 2017 at the foot of Mt. Manthap in the north eastern parts of the country attracted worldwide attention not only because it was the largest after the CTBT mandate but also claimed to be a hydrogen bomb. The seismic signals recorded on the nearby seismological stations were attributed to the main test and its non-tectonic aftershock [Liu et al., 2018], caused by the collapse of the cavity and aseismic compaction. Although most of the detection methods used for underground nuclear tests are based on the seismic methods, Wang et al. [2018] using synthetic aperture radar observations reported the surface displacements upto 3.5 m of divergent horizontal motion and 0.5 m of subsidence associated with the largest North Korean nuclear explosion besides sub-surface collapse and aseismic compaction of the damaged rocks of the test site. Three events on and

after 3rd September 2017 were an earthquake swarm located 8.4 ± 1.7 km north of the nuclear test site within a region of 520 m with depth of at least 2.4 km [Tian et al., 2018]. Two aftershocks of magnitude 2.9 and 3.4 were detected after three months at 0613 and 0640 GMT on 9 December 2018 due to the local readjustments of stresses towards equilibrium. Differences in the estimates of the yield of the largest test in North Korea have been reported [IRIS report, 2017] and therefore larger data set is needed to reconcile such results. Also, discrimination method based on the relation between the body wave magnitude (mb) and the surface wave magnitude (Ms) needs to be examined for North Korea site. In view of the uncertainties in the yield estimation, its variation from the Indian seismic network also needs to be studied. (Figure 1, 2 and 3).

The objective of this paper is to examine the utility of the Indian broadband digital network to monitor the

largest nuclear test of 03 September 2017 by North Korea. Two velocity models namely Crust 2.0 [Bassin et al., 2000] and ak135 [Kennett et al., 1995] have been used to calculate the P-wave anomaly at the Indian stations from this source. Its source parameters have been worked out using full waveform inversion technique. The results have been used to understand the role of tectonic disturbances at the test site which influence not only the source mechanism but also the surface wave magnitude. A comparison of the discriminatory criteria based on the mb versus Ms, Complexity test, Spectral Ratio (SR) and Third Moment of frequency (TMF) have been made. Also the yield (kt) from this test based on the Indian stations data has been compared with that reported elsewhere.

2. LOCAL GEOLOGY AND TECTONICS

The local geology of the North Korean nuclear test site could not be studied due to restraints for field visit by outside agencies. Attempts were therefore, made in USA to utilise the remote sensing data to assess its nature. Lithologic boundary between the geological units were based on the ASTER imagery. The 2006 nuclear test occurred in basement host rock characterised as highly foliated and highly fractured, either Precambrian Saitoku gneiss or could be Melson schistose granite probably of Mesozoic/Jurassic age. The nuclear tests in 2009 and 2013 occurred in a more competent plutonic host rock, either Mesozoic/Cretaceous Tokureido diorite, a very hard rock

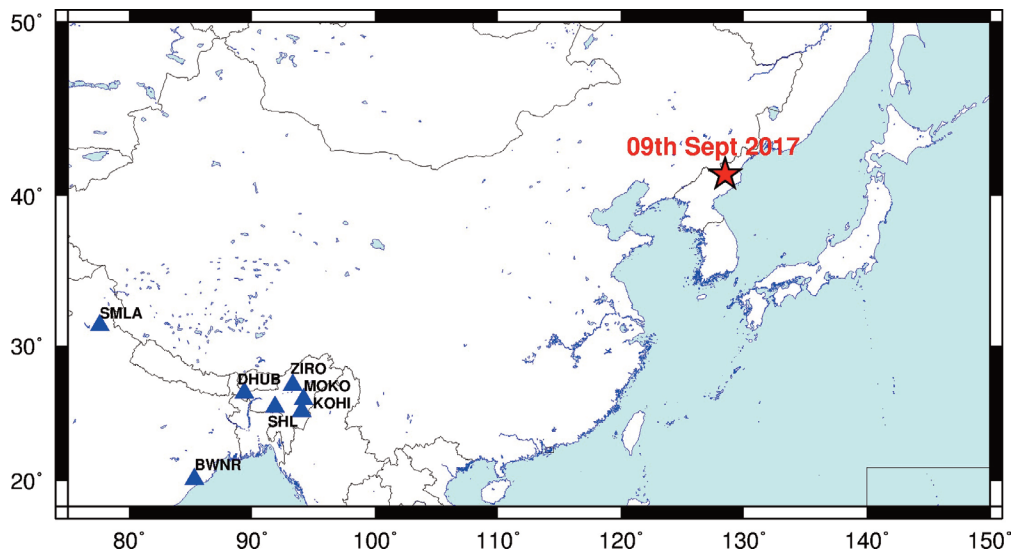


FIGURE 1. Site of the 2017 North Korean nuclear test with reference to Indian Seismological Stations.

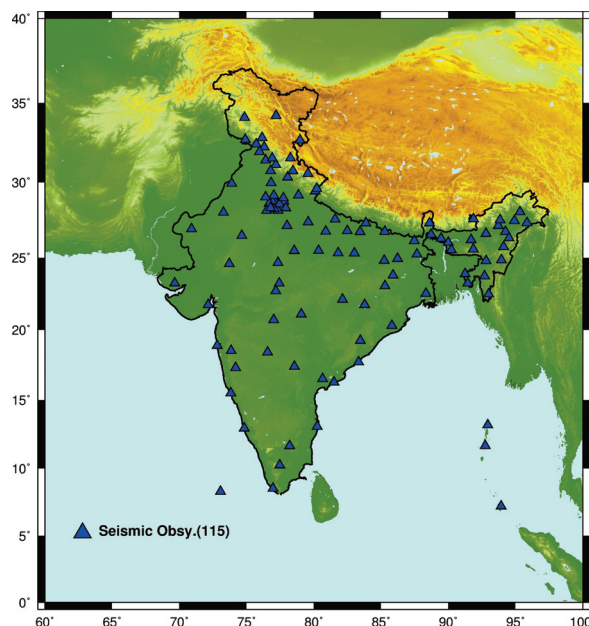


FIGURE 2. Seismic monitoring network of National Centre of Seismology (NCS) (Formerly India Meteorological Department).

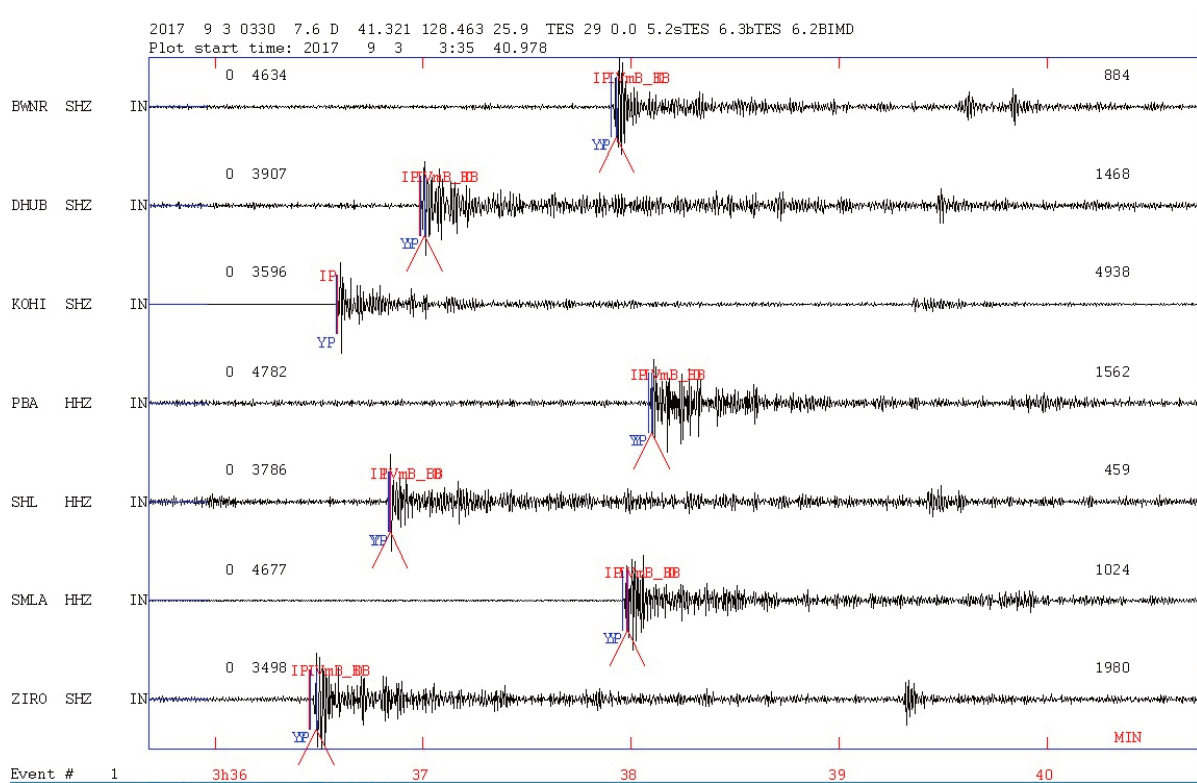


FIGURE 3. Seismograms of the 2017 North Korean nuclear test at selected Indian stations.

comparable to granite or alternatively a less fractured variation of a Mesozoic granite [Coblentz and Frank, 2013]. This provided better containment and coupling. The experience gained from these nuclear blasts enabled North Korea to choose a relatively better basement rock to minimise the leakage of radionuclides as observed after the September 2017 nuclear test. Near Mt. Manthap a NW–SE trending fault was inferred close to Punggye-ri nuclear test. The mountainous region where all the nuclear tests by North America were carried out was seismically less active as compared to Nevada region in USA but somewhat similar to Kazakhstan.

3. DATA AND ANALYSIS

The Epicentral parameters of the six North Korean events as determined by the US Geological survey (USGS) are given in Table 1a. Gibbons et al. [2017] gave relative location estimates for the 5 nuclear test conducted by North Korea up to 2016 using empirical slowness corrections. Kim et al. [2018] estimated average depths of 2006, 2009 and 2013 nuclear tests as 2.12, 2.06 and 2.05 km respectively from the spectra of fundamental Rayleigh wave as well as spectra of depth phases of body waves. These depths were greater than the standard experiment practice. Figure 3, shows the seismograms of the 2017 North Korean nuclear test at selected Indian sta-

tions. It may be noted that P, S and surface waves are well recorded at these stations. The following analysis of the data was carried out:

- P-waves anomalies at the Indian seismological stations due to 2017 nuclear test were analysed using various global models like Crust 2.0 and ak135. The data was also used to determine the epicentral parameters of the largest North Korean nuclear test 2017 (Table 1b). It was found that the model ak135 is a better representation for this source as compared to Crust 2.0 due to negligible P-wave anomaly at the Indian stations (Table 2). The larger anomaly of about 2 seconds based on Crust 2.0 was comparable to Jeffrey-Bullen travel time tables for the Cannikin nuclear explosion [Srivastava and Chaudhury, 1974] which however showed better agreement with the Herrin’s model [Herrin, 1968]. Keeping in view negligible errors in the P-wave anomaly at the Indian stations, the model ak135 was adopted for moment tensor solution as discussed later.
- The moment tensor waveform inversion method is widely used to determine the source properties of earthquakes and the balance between volumetric and non-volumetric strain in the seismic source. The same method has been extended in this paper to study the source characteristics of the largest North Korean nuclear test 2017, based on the Indian seismological stations data. Its fault plane solution was determined us-

ing ISOLA [Sokos and Zahradnik, 2008] after constraining the hypocentral location. The Indian stations used for waveform modelling were ZIRO, KOHI, SHL, DHUB, SMLA, BWNR, and PBA. It may be mentioned that the Indian network is located about 3500 to 5500 km away from the test site, which could result in attenuation of high frequency signals that were observed at close by stations. Keeping this in view, the source characteristics of the 2017 event obtained from the Indian stations have been compared with those based on the stations around and near the test site [Wang et al., 2018]. Wang et al. [2018] found its moment as 9.5×10^{16} Nm giving Mw as 5.24 and 50 to 90 % positive isotropic component and relatively small CLVD or double couple contributions. In contrast, the full wave form modelling results from the Indian stations showed the isotropic component as 16.7 % while the DC and CLVD components were 47.5 and 35.8 % respectively. This difference is attributed to the attenuation of the higher frequencies from the source to the Indian stations.

The methodology for the source mechanism based on a multiple point source representation and iterative deconvolution method [Kikuchi and Kanamori, 1991; Sokos and Zahradnik, 2008] has been discussed by Prakash et al. [2018]. The decomposition in ISOLA for the inversion process namely, volumetric or isotropic (ISO);

compensated linear vector dipole (CLVD) and Double Couple (DC) is based on the methods given by Vavrycuk [2001] and Benetatos et al. [2013]. Thus the principal component in the resultant moment tensor indicates the source property namely explosion, an implosion or a double couple.

In the present analysis, digital data from the broadband Indian stations (Figure 3) was used to model the source parameters of the recent event using ak135 velocity model. The signal to noise ratio was checked to define the proper frequency band for the inversion. The details of constraining the depth of the source below the USGS epicentral location of this event are similar to those described by Prakash et al. [2018] with the filter frequency band of 0.03 to 0.1 Hz and cosine tapering. Moment tensor inversion was then carried out using the data of selected Indian seismological stations as shown in Figure 4. In the multiple source inversion run, trial source orientation was taken as 293° strike, 51° dip and a reference depth of 1km (estimated from single source inversion based on the present study). A grid of 30 trial source positions (10-point source along the strike and 3-point source along the dip with a spacing of 0.5 km) was used. A plot of correlation vs DC% shown in Figure 5a showed well constrained results with DC 47.5% and maximum correlation of 0.7. The final fault plane solution obtained from the inversion of the seismic waveform with their correlation parameter and DC% is shown in Figure 5b.

Date	Time (UTC)	Lat° N	Long° E	Magnitude (mb)	Depth (Km)
2017-09-03	03:30:01	41.343	129.036	6.3	0.0
2016-91-09	00:30:01	41.287	129.047	5.3	0.0
2016-01-06	01:30:01	41.300	129.047	5.1	0.0
2013-02-12	02:57:51	41.299	129.004	5.1	0.0
2009-05-25	00:54:43	41.303	129.037	4.7	0.0
2006-10-09	01:35:28	41.294	129.094	4.3	0.0

TABLE 1a. Epicentral parameters of the Six (6) North Korean nuclear tests (USGS).

S.No.	Date	Origin Time (UTC)	Epicentre	Focal Depth (Km)	Magnitude			Source
					mb	Ms	Mw	
1.	2017.09.03	03:30:07.57	41.321 128.459	1.0	6.3	5.2	5.8	NCS
2.	2017.09.03	03:30:02.00	41.3330 129.0560	0.0	6.3		5.2	NEIC

TABLE 1b. Epicentral parameters of the 3rd September 2017 North Korean nuclear test derived from various agency.

ASSESSING NORTH KOREAN EXPLOSION 2017 THROUGH INDIAN NETWORK

Stn	Dist	AZM	Phase	Hour	Min	sec	Velocity Model (CRUST 2.0)			Velocity Model (AK135)		
							OBS	CAL	Anomaly	OBS	CAL	Anomaly
LKP	3335	252.6	P	3	36	14	367.27	369.12	-1.85	367.27	367.22	0.05
PASG	3347	254.5	P	3	36	15	368.28	370.13	-1.85	368.28	368.24	0.04
ZIRO	3501	255.1	P	3	36	27.3	380.57	382.51	-1.94	380.57	380.61	-0.04
JORH	3519	253.5	P	3	36	28.5	381.78	383.71	-1.93	381.78	381.81	-0.03
MOKO	3525	252.6	P	3	36	29.2	382.5	384.42	-1.92	382.5	382.52	-0.02
TEZP	3644	254.7	P	3	36	38.4	391.67	393.57	-1.9	391.67	391.67	0
IMP	3671	251	P	3	36	40.6	393.94	395.84	-1.9	393.94	393.94	0
SILR	3765	252.1	P	3	36	47.9	401.24	403.09	-1.85	401.24	401.19	0.05
SHL	3788	254.1	P	3	36	49.9	403.22	405.14	-1.92	403.22	403.24	-0.02
DHUB	3910	256.5	P	3	36	59.1	412.41	414.43	-2.02	412.41	412.41	0
SAIH	3910	248.8	P	3	36	59.2	412.5	414.31	-1.81	412.5	412.53	-0.03
SLGI	3996	258.8	P	3	37	5.7	419	420.95	-1.95	419	419.05	-0.05
BOKR	4390	257.2	P	3	37	35.8	449.16	450.99	-1.83	449.16	449.09	0.07
PTH	4508	269	P	3	37	44.8	458.15	460.02	-1.87	458.15	458.12	0.03
BWNR	4636	253	P	3	37	54.1	467.42	469.28	-1.86	467.42	467.38	0.04
SMLA	4680	273	P	3	37	57.4	470.69	472.55	-1.86	470.69	470.66	0.03
DHRM	4693	275	P	3	37	58.6	471.88	473.69	-1.81	471.88	471.81	0.07
SRIN	4721	278.2	P	3	38	0.2	473.47	475.4	-1.93	473.47	473.52	-0.05
PBA	4784	237	P	3	38	4.8	478.09	480.06	-1.97	478.09	478.19	-0.1
BLSP	4808	258.3	P	3	38	6.7	480.02	481.91	-1.89	480.02	480.01	0.01
SONA	4848	269.4	P	3	38	9.5	482.78	484.73	-1.95	482.78	482.84	-0.06
KUDL	4902	269.7	P	3	38	13.5	486.79	488.63	-1.84	486.79	486.74	0.05
KHET	4963	270	P	3	38	17.9	491.17	493.09	-1.92	491.17	491.2	-0.03
VISK	5019	252.4	P	3	38	21.9	495.24	497.11	-1.87	495.24	495.22	0.02
AJM	5155	268.9	P	3	38	31.6	504.89	506.79	-1.9	504.89	504.9	-0.01
LATR	5519	258.8	P	3	38	56.9	530.22	532.13	-1.91	530.22	530.23	-0.01
POO	5734	261	P	3	39	11.7	544.96	546.88	-1.92	544.96	544.98	-0.02

TABLE 2. P-wave anomaly from 2017 North Korean nuclear test at the Indian stations using velocity model crust 2.0 and ak135.

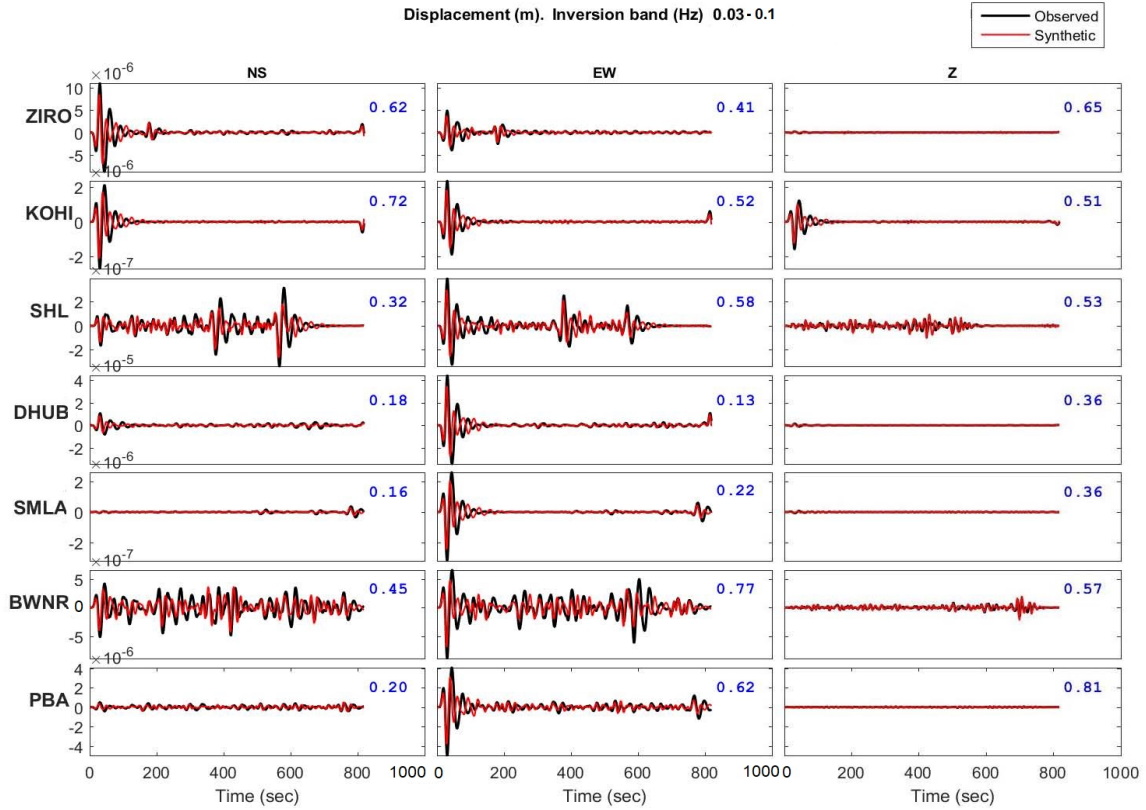


FIGURE 4. Full wave form modelling for source mechanism of the 2017 North Korean nuclear test using Indian stations data.

3.1 DISCRIMINATION TECHNIQUES

Methods to discriminate the nuclear explosions from earthquakes have been generally based on the mb- M_s differences. Of late some other methods like complexity versus spectral ratio, and the differences in the third moment frequency contents (TMF) have also been employed for this purpose. Methods that will be used in this paper are discussed below.

3.1.1 mb VERSUS M_s

Underground nuclear explosions generally release tectonic stress near the site of detonation. Love waves are generated by the tectonic component alone while Rayleigh waves are generated in both the cases whether earthquake or explosion. Thus, the surface wave magnitude becomes an important discriminatory criterion for earthquakes and nuclear explosions. Since Himalayan tectonics due to the fractured lithosphere caused by multiple collisions of the Indian and Eurasian plates lies in the path of seismic waves from the North Korean test site to the Indian subcontinent, it is of interest to work out the relations between mb and M_s for the earthquakes of magnitude 6 or more as well as all the earthquakes recorded by the USGS catalogue for the period 1961 to 2017 in the Himalayan region ($24^\circ - 40^\circ\text{N}$ and $70^\circ - 98^\circ\text{E}$) and

then compare with those of the nuclear tests. Using screening relationship (1), the earthquakes of magnitude 6 and above (Figure 6a) shows that these earthquakes clearly fall above the screening line.

$$M_s = 0.95 \cdot mb - 1.688 \tag{1}$$

However if all the earthquake data that extend to lower magnitudes was taken (Figure 6b), then some earthquakes would found to cross the screening line and located in the nuclear explosion zone. This suggests that the screening line cannot be extended to the lower magnitudes. Also the mb versus M_s plot of the 2017 largest nuclear test lies close to screening line.

The mb and M_s values for the 2013 nuclear test ranged from 4.6 to 5.3 and 3.14 to 4.2 with their mean values as 4.9 and 3.7 at the Keskin SP array (BRTR) station respectively [Semin et al., 2013] and were below the provisional screening line (2) at each array site given by Selby et al., 2012.

$$M_s = mb - 0.64 \tag{2}$$

The magnitude mb given by USGS was slightly larger as 5.1 for the North Korea event.

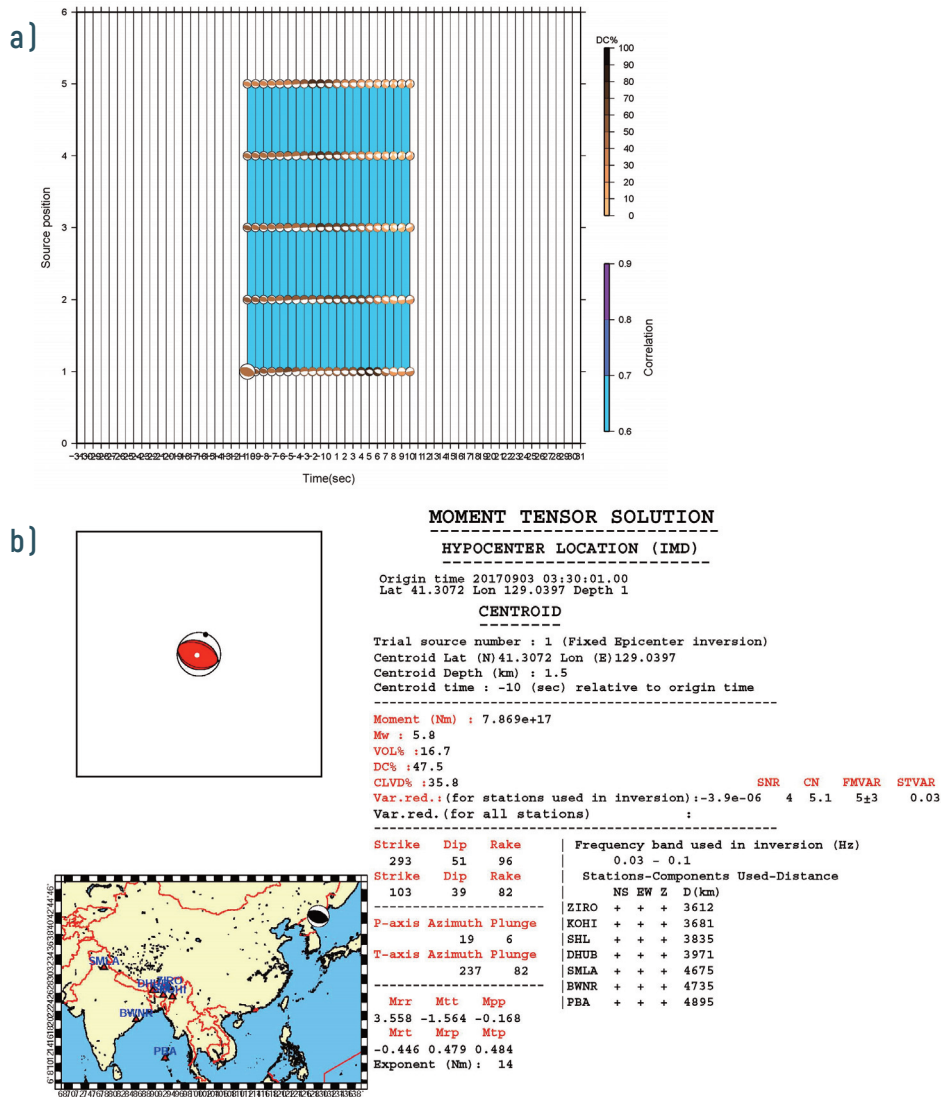


FIGURE 5a). Correlation plot between source position and Time (sec). b) Double couple source mechanism of largest North Korean nuclear test from present study.

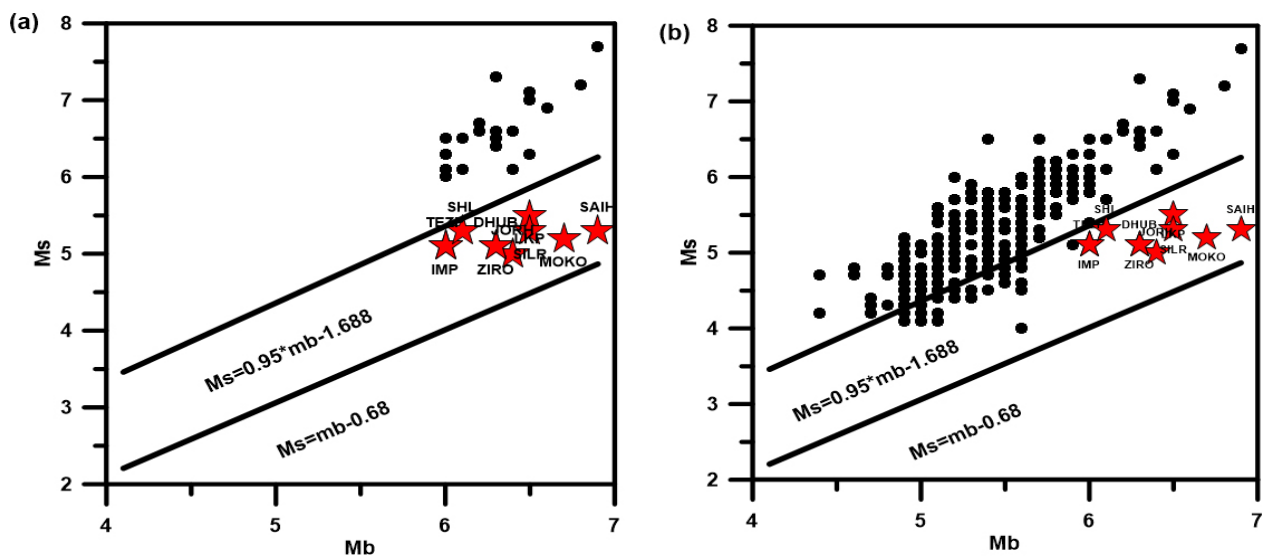


FIGURE 6. (a) mb:Ms plot showing the Himalayan earthquakes $M_w > 6.0$ during 1960–2017 and the mb:Ms values for the explosion (Red star) recorded at Indian Station used in this study. The two dashed lines are the bounding line to the explosion population $M_s = 0.95 * m_b - 1.688$ and the proposed screening line $M_s = m_b - 0.68$. (b) mb:Ms plot showing the Himalayan earthquake during 1960–2017 and the mb:Ms values for the explosion (Red star) recorded at Indian Station used in this study.

Event	Origin time	Longitude	Latitude	Depth	Magnitude	Strike	Dip	Rake	DC%	ISO	CLVD
20170903 (NCS)	03:30:00	129.036	41.343	0.0	6.3 mb	293	51	96	47.5	16.7	35.8
20170903 Han et al., 2017	03:30:01	129.11	41.35	2.4	6.3 mb				26.6	72.3	1.1
20170903 Liu et al., 2018		129.07	41.30	0.5-2.5	6.3 mb				5.6	57.4	37.0

TABLE 3. Source parameters of the 2017 North Korean nuclear test derived from Indian stations.

The variation of mb versus Ms for the largest nuclear test, 2017 at the Indian stations are shown in Figure 6a and 6b. The mean values of mb and Ms from the Indian data were 6.37 and 5.2 respectively. The moment magnitude of this test from the Indian stations was found as 5.8 (Table 4), while much lower value of 5.24 was reported from the close by stations [Wang et al., 2018].

3.1.2 COMPLEXITY (C) TEST

Seismograms of nuclear explosions are much simpler as compared to earthquakes due to generation of mainly compressional waves while they appear more complex due to P as well as S waves in the later. Based on the larger fraction of the total energy in the initial part of the seismograms in the case of nuclear explosions and larger energy centred in the later portion of the seismograms in the case of earthquakes [Gaber et al., 2017] discrimination methods were developed using spectral complexity, waveforms and their amplitudes.

Complexity (C) is defined as the reverse ratio between the energy content within the first five seconds (t_1) of the P-waves to the energy content in the following thirty seconds (t_2) [Kelly 1968; Gaber et al., 2017]. C parameter was computed as follows [Kelly, 1968]. The following equation of Kelly [1968] was used in this study to calculate the C parameter which resamples complexity,

$$C = \frac{\int_{t_1}^{t_2} S^2(t) dt}{\int_{t_0}^{t_1} S^2(t) dt} \tag{3}$$

Where $s(t)$ refers to the signal amplitude as function of time (t) and C is known as the ratio of integrated powers of the vertical component of the velocity seismogram, $S^2(t)$ in the selected time windows length (t_0 , t_1 and t_2), where t_0 is the onset time of P-wave, ($t_0 - t_1$) and ($t_1 - t_2$) are the first- and second-time windows. C value was estimated in a time window ($t_0 - t_1$: 2~5 sec and $t_1 - t_2$: 25~35 sec).

Station	Distance	mb	Ms	Mw
JORH	3522	6.40	5.00	5.90
ZIRO	3504	6.30	5.10	5.70
TEZP	3647	6.00	5.10	5.70
IMP	3674	6.00	5.10	5.80
DHUB	3913	6.30	5.10	6.00
MOKO	3528	6.70	5.20	5.80
SAIH	3913	6.90	5.30	6.10
LKP	3338	6.50	5.50	5.30
SHL	3792	6.10	5.30	5.70
SILR	3769	6.50	5.30	6.40

TABLE 4. mb and Ms and Mw of the 2017 North Korean nuclear test calculated from broadband seismic network of NCS.

3.1.3 SPECTRAL RATIO (SR)

The complexity in the frequency domain is expressed by Spectral Ratio (SR) parameter. It is defined as the ratio of integrated spectral amplitudes $a(f)$ of the seismogram in the chosen frequency bands (high-frequency band h_1 , h_2 and low-frequency bands l_1 and l_2) [Gaber et al., 2017]. It is computed from the following relation [Gitterman and Shapira, 1993],

$$SR = \frac{\int_{h_1}^{h_2} A(f) df}{\int_{l_1}^{l_2} A(f) df} \tag{4}$$

Where h_1 and h_2 represent the high-frequency band while l_1 and l_2 are the low-frequency bands. The best discriminating bands for integration limits are based on the spectra of explosion and earthquake after testing a number of frequency bands. In the present study, we used eight stations which were in the epicentral distances of less than

3500 km for both explosion and earthquake for computing the complexity and spectral ratio parameters for each station. For the calculation of SR, we selected the values for the filters (l_1-l_2): 0.7–1.3 Hz, (h_1-h_2): 1.5–2.1 Hz which performed well. The results of our analysis for both C and SR parameters are given in Table 5. Complexity versus the spectral ratio of each station was plotted for the same station in case of 2017 North Korean explosion and the 2014 Bay of Bengal earthquake (Figure 7).

3.1.4 THIRD MOMENT OF FREQUENCY (TMF)

Third Moment of Frequency (TMF) is defined as [Weichert, 1971],

$$TMF = \frac{\left[\int_0^{f_0} f^3 A(f) df \right]}{\left[\int_0^{f_0} A(f) df \right]} \tag{5}$$

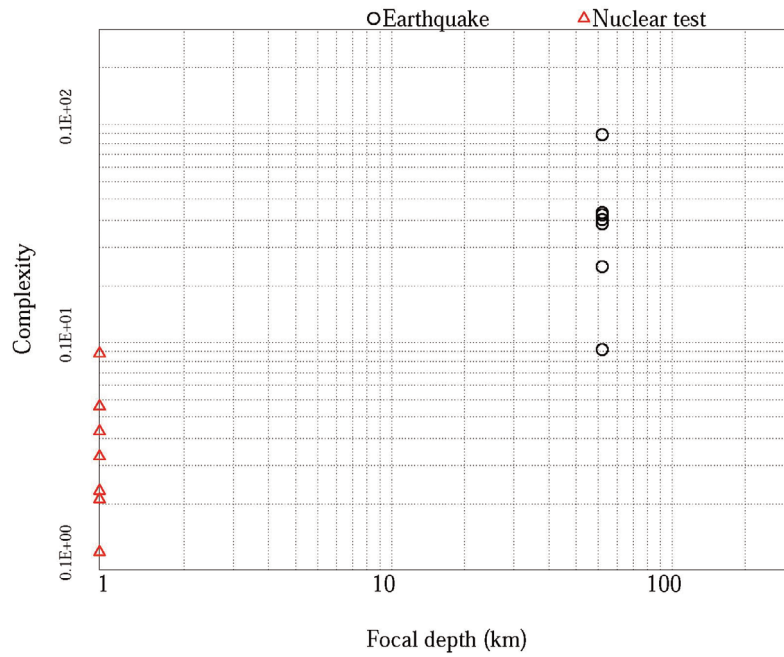


FIGURE 7. Plot of complexity Vs Spectral ratio.

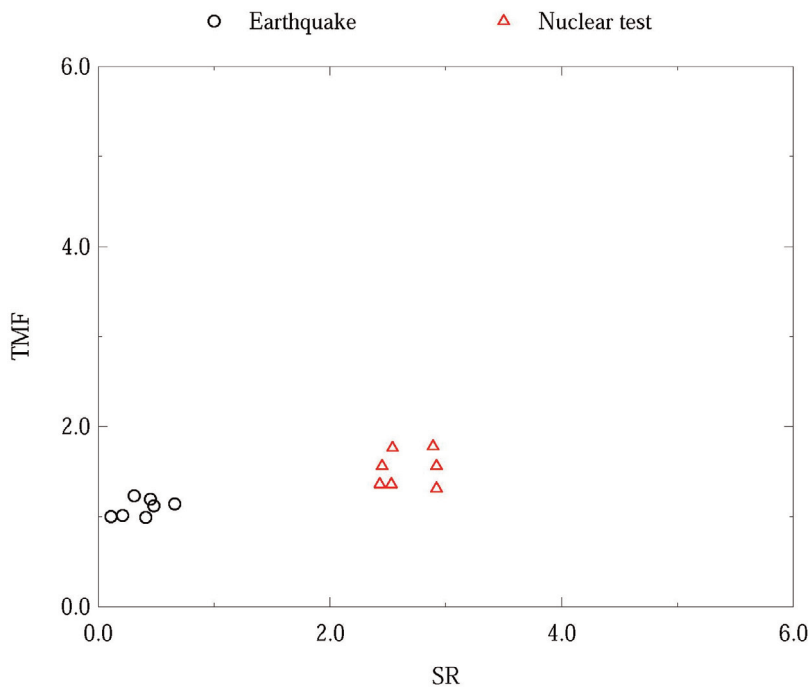


FIGURE 8. Plot of Spectral ratio Vs Third Moment of Frequency.

Where f is expressed in Hz. Since higher weightage is given on the high frequency components in this method, explosions usually give large TMF values.

Various discrimination techniques as given above were used to distinguish the earthquake of May 21, 2014 Bay of Bengal earthquake from the nuclear explosion of September 3, 2017 in North Korea by the help of data collected from the Indian stations. The broadband data was converted into short period using SAC tool and then the instrument response was removed from each station. P-wave Spectra was also calculated from the signals recorded at northeast Indian seismic stations located at distances ranging from about 3500 to 5500 for both North Korea explosion and Bay of Bengal earthquake. The complexity (C), spectral ratio (SR) and Third Moment of frequency (TMF) method was applied to the seismic signals recorded from both the earthquake and the explosion. The relations for the complexity (C) and the spectral ratio (SR) of the 2017 explosion in North Korea and the 2014 earthquake in the Bay of Bengal are shown

in Figure 7 and 8 and Table 5. The results of different methods of discrimination showed that the September 3, 2017 event in North Korea is an underground nuclear test.

3.2 YIELD OF NORTH KOREAN 2017 TEST

As is well known, the correspondence between the seismic magnitude and explosive yield of an underground nuclear test is associated with a very large uncertainty. This is because of the lack of detailed knowledge about basement rock structure, the depth of the test and attenuation characteristics of the medium between the test site and the recording station of the yield.

Some empirical relations between m_b and the yield of the nuclear test are as follows.

Ringdahl et al. 1992 for North America and Eurasia:

$$m_b = 4.45 + 0.75 \log Y \tag{6}$$

where Y is in kilotons.

Station Name	Event Type & Date	Focal Depth (Km)	Complexity (C)	Spectral Ratio (SR)	Third Moment of Frequency (TMF)
ZIRO	EQ, 21 st May 2014	62	9.87	0.21	1.01
KOHI	EQ, 21 st May 2014	62	4.23	0.31	1.23
SHL	EQ, 21 st May 2014	62	3.85	0.41	0.99
DHUB	EQ, 21 st May 2014	62	1.02	0.11	1.00
SMLA	EQ, 21 st May 2014	62	2.45	0.48	1.12
BWNR	EQ, 21 st May 2014	62	4.03	0.66	1.14
PBA	EQ, 21 st May 2014	62	4.33	0.45	1.19
ZIRO	Ex, 3 rd Sept 2017	1	0.98	2.53	1.36
KOHI	Ex, 3 rd Sept 2017	1	0.12	2.45	1.56
SHL	Ex, 3 rd Sept 2017	1	0.23	2.89	1.78
DHUB	Ex, 3 rd Sept 2017	1	0.43	2.92	1.31
SMLA	Ex, 3 rd Sept 2017	1	0.56	2.43	1.36
BWNR	Ex, 3 rd Sept 2017	1	0.21	2.54	1.76
PBA	Ex, 3 rd Sept 2017	1	0.33	2.92	1.56

EQ: Bay Earthquake, 2014
 Ex: North Korea nuclear Explosion 2017

TABLE 5. Complexity (C), Spectral Ratio (SR) and Third Moment Frequency (TMF) calculated for 3rd September 2017 North Korea Explosion and 21st May 2014 Bay of Bengal earthquake.

Murphy [1996] determined the above relation based on the spectra of teleseismic P-waves from the Soviet tests and relative estimates of the attenuation parameters for the western U.S and Central Asia. It gives 0.5 magnitude more in Semipalatinsk as compared to NTS shots of the same yield.

Murphy (1981) for Nevada region:

$$mb = 3.92 + 0.81 \log Y \quad (7)$$

For shots in hard rocks or below water table, it was reported that the test in dry alluvium at NTS may have magnitude 1 unit lower.

Vergino and Mensing [1990] gave the relation:

$$Mb (Pn) = Ar + 0.91 \log Y \quad (8)$$

Where Ar varies between 3.76 and 3.87 for different areas within NTS. This result was suggested for any type of rock including dry alluvium.

Adushkin and Vadim [1993] reported that the measurements from Borovoye station in Kazakhstan can be used to estimate the yields of US explosions to about 20% uncertainty. Khalturin et al. [1998] suggested that the magnitude relation between the teleseismic magnitude and yield is given by

$$mb = 4.64 + 0.73 \log y \text{ (kt)} \quad (9)$$

For a fully coupled explosions

$$Mb = 4.25 + b \log Y \quad (10)$$

Where $b=1$ and Y is greater than 1 [Bowers et al., 2001].

The above relations are discussed later from the Indian stations data.

4. DISCUSSION

The data of close by seismological stations around the 2017 largest nuclear test was used to study its source characteristics by several workers. Liu et al. [2018] found ISO part as 55 to 60 %, CLVD as 30 to 45 % and DC part as 0 to 10 % for this test. However, Han et al. [2017] found slightly different results i.e. ISO 72.3%, DC 26.6% and CLVD 1.1 % with centroid depth of 2.4 km. Wang et al. [2018] found its moment as 9.5×10^{16} Nm giving Mw as 5.24 and 50 to 90 % positive isotropic component and relatively small CLVD or double couple contributions (Table 3). In contrast, the full wave form modelling results from the Indian stations located about 3500 to 5500

km away showed the isotropic component as 16.7 % while the DC and CLVD components were 47.5 and 35.8 % respectively. This difference is attributed to the attenuation of the higher frequencies from the source to the Indian stations. The result of the double couple source mechanism is however similar to that of IRIS report as shown in Figure 5b. Comparison of the source characteristics of smaller North Korean nuclear tests also showed 2009 test to be a non-double couple source [Ford et al., 2009]. However, non-isotropic radiation including shear motion was observed in the 2013 test at the same place [Barth, 2014].

The body wave magnitude of 2017 nuclear test reported by the U.S Geological Survey and China earthquake Centre was 6.3 while it was found as 6.37 from the Indian seismological network. The body wave magnitude of large explosions close to Mb 6.2 (similar to nuclear test, 2017 in North Korea) were reported for eastern Kazakh on 23 June 1979 (6.215), 14 September 1980 (6.213), 27 December 1981 (6.242) and 4 July 1982 (6.222) with their corresponding surface wave magnitudes as 4.26, 4.043, 4.20 and 4.15 [Sykes and Cifuentes, 1984]. Although the values of mb for the Russian nuclear explosions during 1978 to 1982 ranged from 5.576 to 6.242, their Ms varied from 3.637 to 4.106. Adushkin and Vadim [1993] analysed Nevada nuclear tests at a well calibrated station at Borovoye seismic station and found slight difference between mb (International Seismological Centre, U.K.) and that determined from this station. The difference of the results of Kazakhstan and Nevada nuclear test was attributed to differential attenuation of P-waves. The values for the Cannikin [1971], Milrow [1965] and Longshot [1965] in Amchitka islands were 6.8, 6.5 and 6.1 for mb and 5.7, 5.0 and 4.6 for Ms respectively.

Comparison of the smaller North Korean nuclear test (2013) with those of India and Pakistan (1998) of comparable body wave magnitude close to 5 may be interesting due to the different tectonics and path effects. Roy et al. [1998] found the surface wave magnitude as 3.56 for the Pokhran event of 1998 while the mb and Ms of 4.9 and 3.7 were reported for 2013 North Korean nuclear test. Gupta et al. [1999] compared the spectral characteristics of the 1998 Pokhran (India) and Chaghai (Pakistan) nuclear tests and found distinct difference in the energy contents in various frequency ranges. The energy from the Pokhran event was in the frequency range of 3.5 to 6.0 compared to a range of 1 to 3 Hz for the Chaghai explosion showing the influence of the local tectonics. However, this aspect could not be studied for North Korea tests as the Indian stations are located far away.

Baruah et al. [2016] found that similar magnitude earthquake (about 100 km west of the test site) of 2009 and 1998 Indian nuclear test showed that Pn/Lg and

P_n/S_n amplitude ratios of the explosion and the earthquake had distinct differences in the higher frequency window. It was found that the nuclear tests in the North Korea, India and Pakistan and an earthquake (2009) which had m_b of about 5.1 or so produced similar M_s values of around 3.6 for the nuclear tests whereas the earthquake (2009) gave larger M_s (4.3) as could be observed for the Himalayan earthquakes as well. However, the largest North Korean test 2017, gave relatively large surface wave magnitudes at the Indian stations as well as other places as compared to those of Kazakh and Nevada nuclear tests of similar m_b . But they were comparable to nuclear tests of magnitude around 5 in 2013 North Korea, India and Pakistan tests of 1998. It is therefore surmised that larger tectonic slip caused by more powerful fission technology used in 2017 test gave a higher M_s . This was supported by relatively larger component of DC from wave form modelling.

NORSAR estimated the explosive yield at 120 kilotons TNT corresponding to a magnitude of 5.8. On the other hand, Sykes and Cifuentes [1984] reported the yields of seven nearly identical Soviet nuclear tests close to 150 kilotons which were within the limit set by Threshold Test Ban Treaty. The highest yielding test series by the USA and USSR gave yields of 50 megatons. The largest underground nuclear explosion of magnitude 6.8 by the USA called Cannikin gave yield of 5 megatons. On the other hand, the yield estimates of 58+-10 kilotons were estimated for the Indian nuclear explosions in 1998 while the first event in 1974 gave a yield of 12 kt to 13 kt only [Roy et al., 1999]. The yield of the Indian nuclear explosion was estimated as 50 kt from the surface wave magnitude while it was reported earlier as 10 to 50 kt from body waves [Baruah et al., 2016]. Douglas et al. [2001] however estimated much smaller yield of the Indian nuclear explosions. The yields of North Korean tests in 2013 (m_b 5.1), 2009 (m_b 4.7) and 2006 (m_b 4.3) had much lower yields of 7.4 kt, 2.2 kt and 0.65 kt respectively [Semin et al., 2013]. However, Kim et al. [2018] reported 29 kt yield for this test using the relation by Murphy [1981]. While using equations (6) (7), (8) and (9), the yield of the largest North Korean nuclear explosion comes out as 363kt, 1057kt, 737kt and 234kt respectively corresponding to m_b of 6.37 from the Indian stations. Wang et al. [2018] estimated the yield from this nuclear test as 171-209 kt of TNT equivalent for source depths of 350-550 m with best fitting source parameters from geodetic and seismic data. This yield may further increase by 8% if gas porosity in the rocks is doubled. This is somewhat larger as compared to the yields of in Semipalatinsk and Nevada for m_b near 6.2 or slightly more.

The seismic moment was reported as 9.5×10^{16} [Wang

et al., 2018] and 7.86×10^{17} [this study]. The moment magnitude M_w of the largest North Korean explosion was found as 5.8 [present study] and 5.24 [Wang et al., 2018]. Baruah et al. [2016] estimated the M_w of the Indian nuclear test of 1998 as 5.4. Comparison of m_b for the 2017 North Korea test and the 1998 Indian test shows that M_w (5.4) of Indian test was overestimated. No reliable relationship between M_w and yield of a nuclear test is however as yet available which calls for further research.

5. CONCLUSIONS

1. The principal components namely isotropic, DC and CLVD in the moment tensor were found as 16.7%, 47.5% and 35.8% from full wave form modelling from the Indian stations for the North Korean nuclear explosion 2017.
2. The body wave magnitude of the largest North Korean nuclear test was 6.37 from the Indian stations and broadly in agreement with the studies reported earlier. However, the surface wave magnitude of 5.2 from Indian data is larger as compared to that from Kazakhstan and Nevada nuclear tests of similar m_b . But the nuclear test of 2013 in North Korea nuclear test of m_b about 5.1 and M_s 3.6 were comparable to that of Indian test of 1998.
3. The yield of the 2017 largest North Korean nuclear test comes as 363kt, 1057kt, 737kt and 234kt from equation (6) to (9) corresponding to the body wave magnitude (6.37) determined from the Indian stations.
4. Keeping in view similar body and surface magnitudes for North Korean nuclear test of 2013 and 1998 India and Pakistan tests, the tectonics of the region appears to have been changed due to the fusion process in the largest test of 2017. This is also supported by slightly larger DC values from full waveform modelling.

6. DATA AND RESOURCES

Seismograms used in this study were recorded by the observatories maintained by National Centre for Seismology, Ministry of Earth Sciences, New Delhi. The guidelines and procedures to obtain data from IMD are available at www.imd.gov.in and www.isgn.gov.in (both last accessed January 2019). Some plots were made using the Generic Mapping Tools version 5.4.4 (www.soest.hawaii.edu/gmt; Wessel and Smith, [1998]). The earthquake catalogue used in this study obtained from National Centre from Seismology, New Delhi.

Acknowledgements. The authors are grateful to Director, National Centre for Seismology (NCS) for providing the seismological data. One of the authors (SKP) thanks JICA, Japan for providing training on Global seismological observation. This author is also grateful to Dr. Takayuki OTSU, Manager, CTBT National Data Centre, Japan Weather Association for providing useful training for discrimination techniques for earthquakes and explosions. The authors also wish to thank Dr S.N. Bhattacharya, former Head of Seismology, India Meteorological Department for helpful discussions.

REFERENCES

- Adushkin, V.V. and A. An. Vadim (1993). Teleseismic monitoring of underground nuclear explosions at the Nevada test site from Borovoye, Kazakhstan, *Sci. Global Sec.*, 3, 3-4, 289- 309.
- Barth, A. (2014) Significant release of shear energy of the North Korean nuclear test on February 12, 2013, *J. Seismol.*, 18, 605-615.
- Baruah, B., P. Kumar and R. Kumar (2016). Discrimination of Explosion and earthquakes: An example based on spectra and source parameters of the 11th May 1998 Pokhran explosion and the 9th April 2009 earthquake, *J. Geol. Soc. Ind.*, 88,13-21.
- Bassin, C., G. Laske and G. Masters (2000). The Current limits of resolution for surface Wave tomography in North America, *EOS Trans AGU*, F897.
- Benetatos, C.J. and M.F. Verga (2013). Moment tensor inversion for two micro-earthquakes occurred inside the Hájé gas storage facilities Czech Republic, *J. Seismol.*, doi: 10.1007/s10950-012-9337.
- Bowers, D., P.D. Marshal and A. Douglas (2001). The level deterrence provided by data from the SPITTS seismometer array to possible violations of the Comprehensive Test Ban in Noyazemlya region, *Geophys. J. Int.*, 425-438.
- Coblentz, D. and P. Frank (2013). Geologic site characterisation of the north Korean Nuclear Test Site at Punggye-ri: A reconnaissance Mapping Redux *LA-UR-13-29311*, Los Alamos, NM87545.
- Douglas, A., P.D. Marshall, D. Bowers and N.J. Wallis (2001). The yields of the Indian nuclear tests of 1998 and their relevance to Test Ban verification, *Curr. Sci.*, 81, 35-40.
- Ford, S.R., D.S. Dreger and W.R. Walter (2009). Identifying isotropic events using a regional moment tensor inversion, *J. Geophys. Res.*, 114, doi: 10.1029/2008JB005743.
- Gitterman, Y. and A. Shapira (1993). Spectral discrimination of underwater explosions, *J. Earth Sci.*, 42, 37-44.
- Gaber, H., S. Elkholy, M. Abdelazim, I.H. Hamama and A.S. Othman (2017). Seismological investigation of September 09 2016, North Korea, underground nuclear test, *NRIAG J Astro. Geophys.*, 6, 278-286.
- Gupta, H.K., S.N. Bhattacharya, M.R. Kumar and D. Sarkar (1999). Spectral characteristics of the 11 May 1998 Pokhran, and 28 May 1998 Chaghai nuclear explosions, *Curr. Sci.*, 76, 1117-1121.
- Han, L., Z. Wu, C. Jiang and J. Liu (2017). Properties of three seismic events in September 2017 in the northern Korean peninsula from moment tensor inversion, Cornell University Library, arXiv:1710.01586, [physics.geo-ph].
- Herrin, E. (1968). Seismological Tables for P phases, *Bull. Seismol. Soc. Am.*, 58, 1193-1225.
- IRIS Report (2017). Special Event: 2017 North Korean nuclear test, <https://ds.iris.edu/ds/nodes/dmc/special-events/2017/09/03/2017-north-korean-nuclear-test/>
- Kennett, B.L.N., E.R. Engdahl and R. Buland (1995). Constraints on seismic velocities in the earth from travel times, *Geophys. J. Int.*, 122,108-124.
- Kelly, E.J. (1968). A study of two Short-Period discriminants. Technical note, Lincoln Laboratory Massachusetts Institute of Technology U.S.A, 60.
- Khalturin, V.I., T.G. Rautian and P.G. Richards (1998). The seismic signal strength of chemical explosions, *Bull. Seismol. Soc. Am.*, 88, 1511-1524.
- Kikuchi, M. and H. Kanamori (1991). Inversion of complex body waves, *Bull. Seismol. Soc. Am.*, 81, 2335-2350.
- Kim, S.G., Y. Gitterman and S.K. Lee (2018). Depth estimates of the DPRK's 2006-10-09,2009-05-25 and 2013-02-12 underground nuclear tests using local and teleseismic array, *J. Asian Earth Sci.*, doi: 10.1016/j.jseas.2018.05.023
- Liu, J., L. Li, J. Zahradnil, E. Sokos, C. Liu and X. Tien (2018). North Korea 2017 test and its non-tectonic aftershock, *Geophys. Res. Lett.*, doi: 10.1002/2018GL077095.
- Murphy, J.R. (1981). P wave coupling of underground nuclear explosions in various geologic media, in E.S.Husebye and Mykkeltveit S., Identification of Seismic sources Earthquake or underground explosion, 201- 205.
- Murphy. J.R. (1996). Types of seismic events and their source descriptions, in monitoring a comprehensive test ban treaty, in E.S. Husebye and A.M. Dainty, Proc. of the NATO Advanced Study Institute, Kluwer Academic Publishers, Dordrecht. 225-245.
- Ringdahl, F., P.D. Marshall and R.W. Alewine (1992). Seis-

- mic yield determination of Soviet underground nuclear explosions at the Shagan River test site, *Geophys. J. Int.*, 109, 65–77.
- Roy, F., G.J. Nair, T.K. Basu, S.K. Sikka, A. Kakoddddkar, R. Chidambaram, S.N. Bhattacharya and V.S. Ramamurthy (1999). Indian explosions of 11 May 1998: Analysis of regional Lg and Rayleigh waves, *Curr. Sci.*, 76, 1669–1673.
- Selby N.D., P.D. Marshall and D. Bowers (2012). Mb:Ms event screening revisited, *Bull. Seismol. Soc. Am.*, 102, 88–97.
- Semin, K., O. Necmioglu, C. Destici, N. Ozel, S. Kocak and U. Teoman (2013). The analysis of DPRK nuclear test of February 12, 2013 by Belbasi nuclear tests monitoring centre- Korea, Science and Technology Conference, Bogazici University, Istanbul, Turkey.
- Sokos, E.N. and J. Zahradník (2008). ISOLA a FORTRAN code and a MATLAB GUI to perform multiple-point source inversion of seismic data, *Comput. Geosci.*, 34, 967–977.
- Srivastava, H.N. and H.M. Chaudhury (1974). P wave anomalies from CANNIKIN at the Indian stations, *Bull. Seismol. Soc. Am.*, 64, 1329–1335.
- Sykes, L.R and I.L. Cifuentes (1984). Yields of Soviet underground nuclear explosions from seismic surface waves: Compliance with the threshold test ban treaty, *Proc. Natl. Acad. Sci., USA*, 81, 1922–1925.
- Tian, D., J. Yao and L. Wen (2018). Collapse and earthquake swarm after North Korea's 3 September 2017 nuclear test, *Geophys. Res. Lett.*, 45, 3976–3983. <https://doi.org/10.1029/2018GL077649>.
- Vavrycuk, V. (2001). Inversion for parameters of tensile earthquakes, *J. Geophys. Res: Solid Earth*, 106, 16339–16355.
- Vergino, E.S. and R. W. Mensing (1990). Yield estimation using regional mb (Pn), *Bull. Seismol. Soc. Am.*, 80, 656–674.
- Wang, T., Q. Shi, M. Nikkhoo, S. Wei, S. Barbot, D. Dreger, R. Burgmann, M. Motagh, and Q. F. Chen (2018). The rise, collapse and compaction of Mt. Mantap from the 3 September 2017 North Korean nuclear test, *Science*, doi: 10.1126/science.aar7230
- Weichert, D.H. (1971). Short period spectral discriminant for earthquakes and explosion differentiation. *Geophys.*, 37, 147–152.

*CORRESPONDING AUTHOR: Sanjay Kumar PRAJAPATI,
National Centre for Seismology, New Delhi, India
email: go2sanjay_p@yahoo.com